# Growth of polyhedral stacked micro columns and micro particles of zinc by thermal evaporation and condensation technique

Rivera-Flores B. L.*, Díaz-Becerril T., Bueno-Avendaño C., Galeazzi-Isasmendi R., Rosendo-Andrés E., García-Salgado G., Juárez-Santiesteban H., Pacio-Castillo M., Morales-Ruiz C.
*CIDS-ICUAP, Benemérita Universidad Autónoma de Puebla*
*Av. San Claudio y 14 Sur s/n, Edif. 103-C, Puebla, Pue. 72570, México*

Silva-González R.
*Instituto de Física, Benemérita Universidad Autónoma de Puebla*
*Apdo. Postal J-48, Puebla, Pue. 72570, México*
(Recibido: 9 de abril de 2014; Aceptado: 4 de julio de 2014)

Metallic zinc nanostructures have been grown by the thermal evaporation and condensation technique using a mixture of zinc and manganese oxide powders and nitrogen as carrier gas. 650 °C and 1 atm were used as processing temperature and pressure, respectively. It was found that the shape of zinc structures is dependent on the source materials. When a mixture of $Zn/MnO_2$ powders is used as raw material micro-particles with oblate spherical shape and micro-columns are obtained. On the other hand, when only zinc powder is used as source material, spherical stones without facets are deposited. It is assumed that evaporation from the source is inhibited when a mixture of Zn and $MnO_2$ is used. Therefore, supersaturation downstream from the source changes and as a consequence the morphology of the structures is modified. Synthesized material is make-up of zinc atoms and no other impurities or catalytic particles were detected according to elemental analysis. Vapor–solid is though as mechanism for growing those zinc structures.

*Keywords:* Zinc microstructures; Evaporation-Condensation Technique; Hexagonal Zinc

## 1. Introduction

Growth of low dimensional nanostructures is of great interest in both scientific and technological point of view because of their novel electronic properties. In addition, such nanostructures are considered to be the building blocks for nanoscale electronic and optoelectronic nanodevices.

Many efforts have been done to synthesize nanosized structures of several kinds of materials, including metals [1-3], semiconductors [4-6] and metal oxides [7-9]. Metallic nanostructures have shown enhanced properties that might be applied in catalysis, electronic and storage devices [10-12]. Specifically, Zn nanostructures are of particular interest due to their noticeable features and it is considered as good candidate to fabricate batteries [13-14]. In this regard, Zn nanowires have shown enhanced thermopower characteristics [15] and also exhibit superconductivity [16]. In addition, Zn nanowires are considered as candidates for building metallic interconnections of devices in the future nanoscale electronics. Additionally, zinc is an important precursor for preparation of other Zn-based semiconductors such as ZnO, ZnS, and ZnTe, which have extensive applications in electronics, photonics and photoelectronics.

Among the methods for synthesizing Zn nanostructures are electron beam irradiation, thermal evaporation, electrodeposition, and others [17-20].

Thermal evaporation–condensation growth, also referred as vapor-solid process, is commonly used to synthesize one and two dimensional nanoscale shapes of metallic zinc [21-23]. It is well known that the morphologies of the synthesized material grown by this technique have strong dependence on the experimental parameters. The level of supersaturation of the growth species in the gas phase is one of them. Under advection condition, it exist a maximum in the vapor concentration and the supersaturation decreases from the source material. The localization of this maximum along the furnace will shift downstream as the carrier gas flow rate increases [24]. The starting material used as source also might change the concentration of the growth species in the vapor phase and therefore, the resulting morphology of the obtained nanostructures [18, 25-27].

In this work, thermal evaporation-condensation approach was used to synthesize Zn structures. This material was obtained evaporating a mixture of Zn and $MnO_2$ powders in a conventional horizontal furnace heated to 650 °C. For comparison, Zn structures were also grown under the same experimental conditions by using Zn powders as source. The material was collected and characterized by X-ray diffraction (XRD), energy dispersive X-ray spectroscopy (EDS) and scanning electron microscopy (SEM) techniques.

Different morphologies were obtained depending on the material used as source. Micro-columns and micro-particles with oblate spherical shape were deposited on the substrate when a $Zn/MnO_2$ mixture was evaporated. Neither, evidence of inclusion of Mn in the grown Zn structures, nor formation of a $MnO_2$ phase was observed.



* dubhe_1@yahoo.com.mx

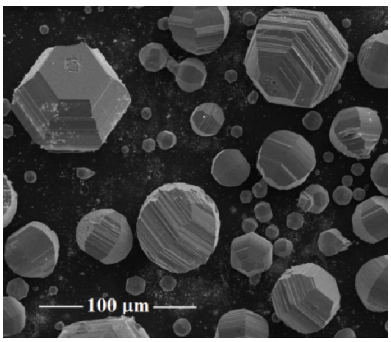


(a)

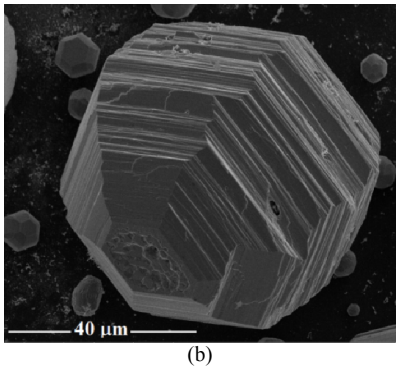


(b)

**Figure 1.** Particles with spherical oblate shapes grown on the quartz substrate. (a) SEM top view. (b) A closer view of the particle showing its apparent hexagonal plate.

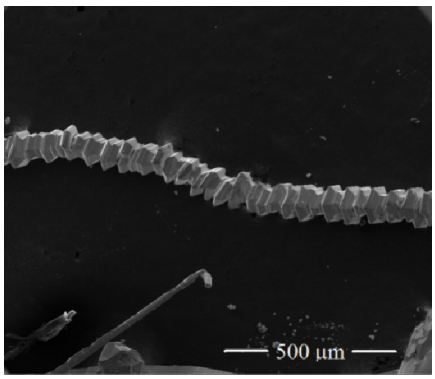


(a)

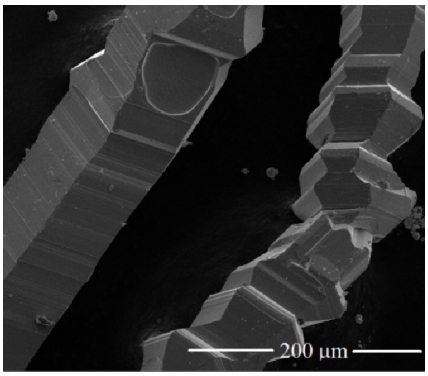


(b)

**Figure 2.** SEM pictures of micro-columns-like. (a) A top view and (b) A detailed photograph showing the stacked micro-particles that is made of.

On the other hand, when Zn was used as source, spherical Zn particles were obtained. In the light of the experimental evidence, the addition of $MnO_2$ powder as precursor changes, to some extent, the shape and size of the growth material. A possible growth mechanism of such structures is sketched.

## 2. Experimental

The zinc microstructures were prepared using thermal evaporation and condensation technique under controlled growth conditions. The experimental set-up used for the synthesis consisted of a horizontal quartz tube furnace heated by an electrical resistance, a temperature controller, a quartz one-side opened reactor and an inert gas supply with control flow system.

A mixture of Zn (99.9%) and $MnO_2$ (99.9%) powders in a molar ratio of 10:0.5, 10:0.25, 10:0.0 were used as source materials. Each mixture was put in a quartz boat and inserted into the reactor. A quartz plate used as substrate was placed at 25 cm from the center of the boat downstream of the gas flow and then the reactor was sealed with a silicon lid.

The furnace was heated up to 650 °C and then the reactor was introduced quickly into the furnace, from room temperature, and kept there for 60 min under a constant nitrogen flow. The gas carrier was introduced into the reactor through a mass-flow controller at rate of 30 standard cubic centimeters per minute (sccm). After 60 min of process the electrical resistance was turned off but the reactor remained into the furnace till it reached the room temperature. After that the nitrogen flow was stopped.

The synthesized products were characterized in microstructure, morphology, and chemical composition using X-Ray Powder Diffraction (XRD) with a BRUKER AXS-D8 Discover (Cu K" radiation) diffractometer, Scanning Electron Microscopy (SEM) with a FEI Helios-Nanolab 600 SE microscope, with X-Ray Energy Dispersive Spectroscopy (EDS) analysis attached.

## 3. Results and Discussion

Figure 1 shows SEM micrographs of as synthesized Zn material on quartz substrate. Two different morphologies were observed depending on their position on the substrate. Zone 1 running from 25 to 31 cm from the centre of the boat (temperatures from 575 to 520 °C) particles with oblate spherical shape were grown, as shown SEM images in figures 1a and 1b. The diameter of such particles ranged from 5 µm to 50 µm. The oblate spherical particles seem to be composed by hexagonal plate stacks having a thickness of 50 nm approximately. On the other hand, micro-columns composed by stacked polyhedral micro-particles are seen (figure 2a) in zone 2 placed between 31 and 35 cm from the source. These micro-particles also seem integrated by hexagonal plates as observed in figure 2b. Micro-columns are around 60 µm in diameter and hundred microns in length.

**Table 1**. EDS analysis from structures grown on quartz substrate.

| Growth Zone | Element | Wt % | At % |
|---|---|---|---|
| 1 | O K | 1.85 | 7.17 |
| | Zn K | 98.15 | 92.83 |
| 2 | O K | 1.93 | 7.43 |
| | Zn K | 98.07 | 92.57 |
| 1 | O K | 1.68 | 6.54 |

Crystallinity and phase purity of those particles were analyzed by XRD measurements and their diffraction patterns pictures presented in figure 3. The XRD patterns exhibit five peaks at 2θ = 36.26, 39.05, 43.19, 54.25 and 70.03 and corresponding to Zn crystallized as wurtzite (JCPDS # 04083) with lattice parameter a=b=2.665 Å and c=4.954 Å. Neither signals corresponding to other impurities such as Mn were detected.

From the diffraction patterns of figure 3, lattice parameters of the structures were obtained to be a=b=2.663 Å and c= 4.954 Å which are in good agreement with the values in bulk. It is evident in the XRD spectra that the peak with maxima intensity is the (002) plane corresponding to basal plane of a hexagonal plate [26]. The sharp and narrow peaks imply good crystalline quality of the structures.

$Mn^{+2}$ ions have an ionic radius (0.66 Å) larger than $Zn^{+2}$ (0.60 Å) by four fold coordinating. Therefore, if Mn ions replace Zn ions in the crystal it causes a significant change in the lattice constant resulting in a measurable shift in the (101) and (002) peaks [28-30]. This is not the case, same position peaks were observed independently of the Zn:$MnO_2$ ratio used as source. This fact points out, in this experiment, the growth of this type of Zn structures underwent no detectable lattice change.

The EDS measurements done on some places of the micro-columns and micro-spherical particles give us no evidence of the inclusion of Mn atoms into the Zn structure as is displayed in Table 1. As shown in Table 1, zinc atoms principally compose those structures. A small percentage of oxygen atoms are observed but they could have been introduced during the exposition of the structures to the room environment or by the residual oxygen in the growth chamber forming oxides of Zn.

From the above results, neither XRD nor EDS technique give us evidence of the inclusion of Mn atoms into the Zn matrix for all the different ratios of Zn:$MnO_2$ used in this experiment. Although it is reported doping Mn ions to a detectable level by vapor phase synthesis is extremely difficult [31].

The vapor-solid (VS) mechanism is a catalyst-free process. The growth usually proceeds *via* the evaporation of solid precursors, metallic Zn and $MnO_2$ powders in this case, and consequent condensation of the vapor phase again into a solid phase directly onto the substrates and they grow into nanostructures as observed in figures 1 and

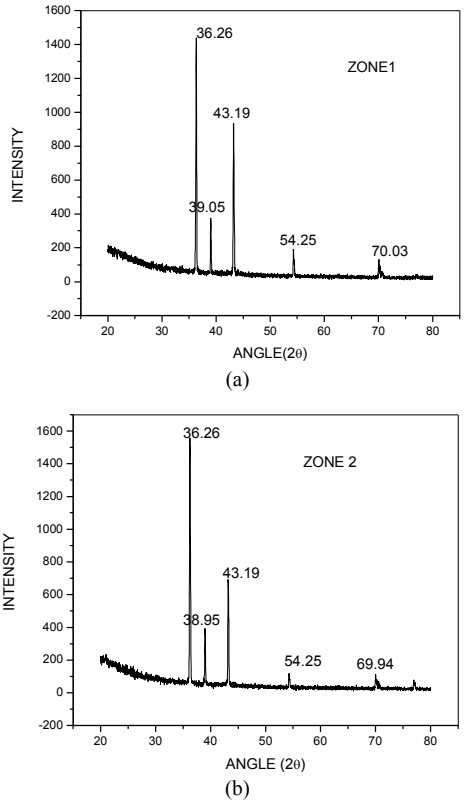


**Figure 3. .** Diffraction patterns obtained from (a) Spherical micro-particles and (b) Micro-columns-like.

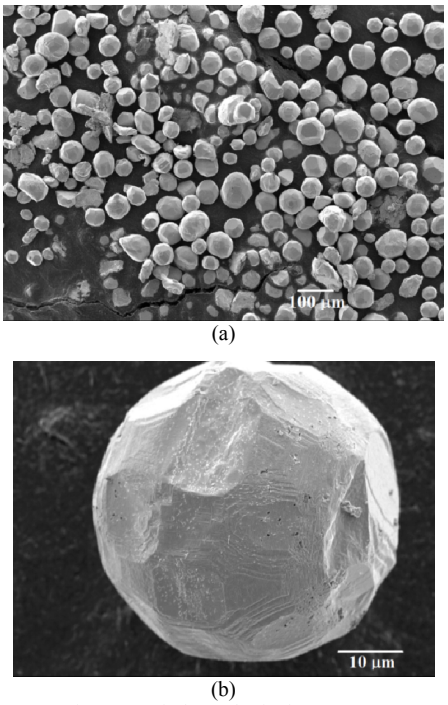


**Figure 4.** SEM images of the spherical stones grown when zinc powders were used as source. (a) A top view and (b) spherical stones.

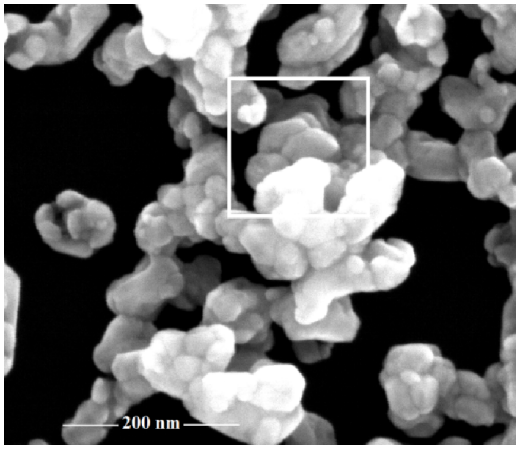


**Figure 5.** A growth in an early stage. SEM picture showing the formation of faceted particles. These particles grow in stack (in the box). Same trend can be seen in other parts of the micrograph

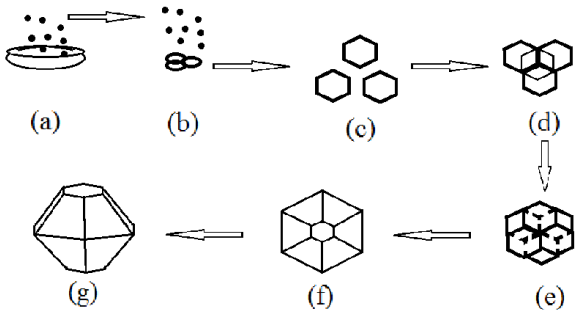


**Figure 6.** Proposed mechanism of growth for spherical oblate particles (a) Evaporation of source material, (b) vapour transport and condensation forming small nuclei and particles, (c) particles became faceted in hexagonal shape, (d) new hexagonal plates are formed, by vapour condensation, on a hexagonal plate already grown. The base plate is drawn in thinner line. New plates are grown over the previous ones (in dashed lines) and a faceted structure is delineated. Finally the growth ends and a spherical oblate particle is obtained (f) a top and lateral (g) representation.

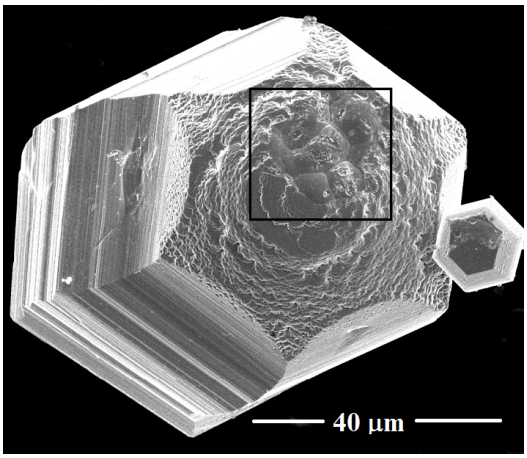


**Figure 7.** SEM image showing the faceted microparticle. The box shows smaller faceted particles that compose it.

2. From the XRD and EDS results given above the presence of other impurities or catalytic particles have been ruled out. Hence, it is thought the growth of these structures is conducted by a VS mechanism.

Different morphology of the material was obtained when the experiments were done using Zn as source without any trace of $MnO_2$ as shown in figure 4. Spherical stones instead of spherical oblate polyhedral are obtained.

These results induce us to think that the Mn might play a role in the formation of the obtained microstructures by modifying the saturation condition on the growth zone under the same experimental conditions.

It is generally believed that growth temperature and gas-phase supersaturation determine the growth rate of surface planes and final morphology of the crystals with other experimental parameters playing minor roles.

It is well stated that to grow nanostructures a supersaturation is needed and the crystal grows under conditions of no thermal equilibrium. In such conditions the growth kinetics takes a part or even determines the growth behavior of the surface planes and from here the final morphology of the structure [24].

The difference in morphology found between the two experiments might be due to a change in the supersaturation of vapor in the furnace while other parameters of the process are kept constant. This means the presence of $MnO_2$ may have a role in changing the evaporation rate of the zinc.

To corroborate this fact, a measurement of the weight of the source after the process was performed. Table 2 displays the weight of the mixtures used as source and the respective weight of the remainders after the process.

As can be seen more material is evaporated when $MnO_2$ is added to Zn. This could lead to a increasing in the vapor concentration along reactor causing different morphology in the growth of structures as seen from figures 1 and 4.

L. W. Yang et al [32] in their experimental work to synthesize Mn-doped ZnO by evaporating a mixture of Zn and $MnO_2$ powders at 700 ˚C found that, Mn ions can effectively affect the growth way of the ZnO structures, which is in agreement with our results.

The growth mechanism of the microstructures can be pictured as follows. Firstly, the vapor atoms condensate on the substrate and forms clusters of Zn. The clusters became faceted forming hexagonal plates and they stacked each other (as shown in the box in the image of figure 5) and a line of stacked hexagonal plates is obtained as a result.

It is known zinc has an hexagonal crystal structure with six-fold symmetry around the c axis. The surface energy of the $\{10\bar{1}0\}$, $\{10\bar{1}1\}$ planes are higher than the surface energy of the $\{0001\}$ planes [33]. Planes with higher surface energy grow faster than other planes to minimize the surface energy of the growing structures.

Therefore, the Zn nuclei grow fast along $\pm[10\bar{1}0]$, $\pm[01\bar{1}0]$, $\pm[1\bar{1}00]$ directions and form hexagonal crystal bounded by low surface energy $\{0001\}$ plane.

The hexagonal faceted plates when stacked form steps that introduce dislocations that acts as favorable sites for

**Table 2.** Quantity of material evaporated from the mixture used as source. The experiments were done in several times to check the results.

| **Molar Ratio Zn:$MnO_2$** | **Total Weight in the Source** (g) | **Total Evaporation** (g) | **Evaporation Temperature** (˚C) |
|---|---|---|---|
| 10:0.50 | 6.895 | 1.4116 | 650 |
| 10:0.25 | 6.713 | 1.2527 | 650 |
| 10:0.25 | 6.713 | 1.3674 | 650 |
| 10:0.25 | 6.713 | 1.2685 | 650 |
| 10:0.00 | 6.542 | 0.48 | 650 |
| 10:0.00 | 6.542 | 0.44 | 650 |
| 10:0.00 | 6.542 | 0.68 | 650 |

Zn atoms to condense from the vapor phase and these hexagonal plates will grow along of fast growing directions and, finally, some poly hedral particles might growth as seen in figure 2. It is worth to point out that each stack on the structure may not be composed by one single hexagonal plate but by several of them and therefore forming irregular shaped polyhedral particles as seen in figure 2.

On the other hand, spherical oblate polyhedral may be grown by a similar way. Zinc atoms from the source are evaporated and carried downstream in gas phase condensate to form hexagonal plates (figure 6 (a), (b), (c)).

On the basal surface of each plate may grow others hexagonal plates figure 6(d). This hexagonal steps formed on the basal planes introduce favorable sites for condensing zinc atoms. On this surface of each already formed hexagon others are grown and the entire structure may become faceted as is drawn in figure 6(e). The process continues and a spherical faceted micro-particle is grown (figures 6(f), 6(g)). As these types of micro-particles are grown at higher temperature than the columns, the Zn atoms have high mobility to move themselves at kinks and steps.

Higher supersaturation allows growing bigger sized particles as shown in figure 1. W. S. Khan et al. [26] proposed a similar growth process for their polyhedral micro-particles but they assume the growth of a single hexagonal plate on each layer of their stack. In our case we are proposing that several hexagonal plates compose each layer of the staked polyhedral. As seen in figure 7 where SEM picture taken on a particle shows three faceted particles embedded in it.

## 4. Summary

It is used the thermal evaporation-condensation technique to synthesize zinc nanostructures. A mixture of Zn and $MnO_2$ powders in a molar ratio Zn:$MnO_2$ of 10:0.50, 10:0.25 and 10:0.0 was used as source. The morphology of the synthesized structures was found to be dependent on $MnO_2$ content. Oblate spherical micro-particles and micro-columns composed by stacked polyhedral particles were obtained as final product when a mixture of Zn:$MnO_2$ was used as source. Those polyhedral particles seem to be composed by stacked hexagonal plates with nanometer dimensions.

Spherical stones without any facets were obtained when zinc powders without $MnO_2$ (molar ratio 10:0.0) was used as source.

X-ray diffraction taken from samples showed consistent patterns verifying that the polyhedral Zn particles are crystalline. Neither XRD nor EDS detected any evidence of inclusion of Mn atoms in the structures or the existence of other phase or impurities. Vapor-solid (VS) it is believed as mechanism to grow these types of structures.

Although no conclusive studies were done it seems the role of the use of $MnO_2$ in the Zn source increases the concentration of zinc atoms in gas phase. This fact might be responsible for the difference in morphology of the structures when they are grown using Zn only as source or when $MnO_2$ is added to it.

Based on a previous work in literature and SEM pictures of the material a mechanism for particles formation is presented.

## References

[1]. M. Hu, J. Chen, Z.-Y. Li, L. Au, G. V. Hartland, X. Li, M. Márquez, Y. Xia, Chem. Soc. Rev. 35, 1084 (2006).
[2]. J. Siegel, O. Lyutakov, V. Rybka, Z. Kolská, V. Švorčík, Nanoscale Res. Lett. **6**, 96 (2011).
[3]. B. Wiley, Y. Sun, Y. Xia, Acc. Chem. Res. **40**, 1067 (2007).
[4]. N. Chekurov, K. Grigoras, A. Peltonen, S. Franssila and I. Tittonen, Nanotechnology **20**, 065307 (2009).
[5]. C. Y. Nam, D. Tham, J. E. Fisher, Appl. Phys. Lett. **85**, (23) 5676 (2004).
[6]. M. Ichikawa, IEEE Journal of Quantum Electronics **38**, (8) 988 (2002).
[7]. Z. L. Wang, Zinc Oxide Bulk Thin Films and Nanostructures, Chapter 10 Ed. C. Jagadish and S. Pearton, Elsevier.
[8]. Ü. Özgür, Ya. I. Alivov, C. Liu, A. Teke, M. A. Reshchikov, S. Doğan, V. Avrutin, S.-J. Cho, H. Morkoç, J. Appl. Phys. **98**, 041301 (2005).
[9]. D. N. Castillo, T. Díaz, E. Rosendo, H. Juárez, G. García., Materials Research Society **1371**, 33 (2012).
[10]. J. M. Sieben, M. M. E. Duarte, International Journal of Hydrogen Energy **36**, (5) 3313 (2011).
[11]. X. Zhang, G. Wang, W. Zhang, N. Hu, H. Wu, B. Fang, J.

Phys. Chem. C **112**, 8856 (2008).
A. S. Aricò, P. Bruce, B. Scrosati, J.-M. Tarascon, W. Van Schalkwijk, Nature Materials **4**, 366 (2005).
[12]. E. Deiss, F. Holzer, O. Hass, Electrochim. Acta, **47**, 3995 (2002).
[13]. Y. Ito, M. Nice, R. Plivelich, J. Power Sources **196**, 2340 (2011).
[14]. J. P. Hermans, C. M. Thrush, D. T. Morelli, M. C. Wu, Phys. Rev. Lett. **91**, 076804 (2003).
[15]. J. G. Wang, M. L. Tian, N. Kumar, T. E. Mallouk, Nano Lett. **5**, 1247 (2005).
[16]. X. Y. Zang, J. Y. Dai, C. H. Lan, H. T. Wang, P. A. Webley, Q. Li, H. C. Ong, Acta Materialia, **55**, 15939 (2007).
[17]. C. F. Guo, Y. Wang, P. Jiang, S. Cao, J. Miao, Z. Zhang and Q. Lin, Nanotechnology **19**, 445710 (2008).
[18]. J. Li, X. Chen, Solid State Commun. **131**, 769 (2004).
[19]. J. Gong, S. Yang, H. Huang, X. Zhao, Z. Z. Yu, Nanotechnology **18**, 235606 (2007).
[20]. J. Liu, Z. Zhang, X. Su, Y. Zhao, J. Phys. D: Appl. Phys. **38**, 1068 (2005).
[21]. F. Ramos-Brito, C. Alejo-Armenta, M. García-Hipólito, E. Camarillo, J. Hernández, C. Fálcony, H. Murrieta, Journal of Luminescence **131**, 874 (2011).
[22]. Y. Zhang, F. Zhu, J. Zhang, L. Xia, Nanoscale Res. Lett .**3**, 201 (2008).
[23]. J. I. Shulin, Y. E. Changhui, J. Mater. Sci. Technol. **24**, (4) 457 (2008).
[24]. Khan, W. M. Jadwisienczak, M. E. Kordesch, Phys. E. **33**, 331 (2006).
[25]. W. S. Khan, C. Cao, Z. Usman, S. Hussain, G. Nabi, F. K. Butt, Z. Ali, T. Mahmood, N. A. Niaz, Mat. Res. Bulletin **46**, 2261 (2011).
[26]. Y. J. Chen, B Chi, H. Z. Zhang, H. Chen, Y. Chen, Materials Letters **61**, 144 (2007).
[27]. F. K. Shan, B. I. Kim, G. X. Liu, J. Y. Sohn, W. J. Lee, B. C Shin, Y. S. Yu, J. Appl. Phys. **95**, (9) 4772 (2004).
[28]. H.-W. Zhang, E.-W. Shi, Z.-Z. Chen, X.-C. Liu, B. Xiao, J. Appl. Phys. **45**, (10A) 7688 (2006).
[29]. X. Zhang, Y. Zhang, Z. L. Wang, W. Mai, Y. Gu, W. Chu, Z. Wu, Appl. Phys. Lett. **92**, 162102 (2008).
[30]. J. Zhang, F. Jiang, S. Ding, Appl. Phys. A **109**, 255 (2012).
[31]. L. W. Yang, X. L. Wu, G. S. Huang, T. Qiuand, M. Yang, J. Appl. Phys. **97**, 014308 (2005).
[32]. P. X. Gao, C. S. Lao, Y. Ding, Z. L. Wang, Adv. Funct. Mater. **16**, 53 (2006).